

# Characteristics of Mg<sub>2</sub>Si – MnSi<sub>x</sub> uni-couple thermoelectric devices

Rishikesh Kumar<sup>1</sup>, Saravanan Muthiah<sup>2</sup>, Avinash K. Singh<sup>1</sup>, Ajay Dhar<sup>2\*</sup>

<sup>1</sup>Noida International University, Gautam Budh Nagar, Uttar Pradesh 203201, India

<sup>2</sup>CSIR-Network of Institutes for Solar Energy, CSIR-National Physical Laboratory, New Delhi 110012, India

\*Corresponding author. Tel: (+91) 11-4560 9456; Fax: (+91) 11-4560 9310; E-mail: adhar@nplindia.org

Received: 06 August 2015, Revised: 03 February 2016 and Accepted: 22 May 2016

## ABSTRACT

We report the synthesis of both n-type Mg<sub>2</sub>Si and p-type MnSi<sub>1.73</sub> using reaction sintering employing spark plasma sintering (SPS) process. The thermoelectric device was fabricated using these synthesized thermoelectric materials having a ZT value of ~ 0.7 for n-type Mg<sub>2</sub>Si and ~ 0.55 for p-type MnSi<sub>1.73</sub>. The two design combination of unicycle thermoelectric devices were fabricated; nickel contacts at hot & cold ends in first device and graphite contact at hot end & nickel contact at cold end in another device. The device comprised of n-type Mg<sub>2</sub>Si & p-type MnSi<sub>1.73</sub> legs each with dimensions of 4 × 4 × 10 mm. The voltage and current output characteristics of this thermoelectric device were evaluated at temperature gradient between hot and cold ends in the range of 50 to 350 K. The maximum open circuit voltage output (~135mV) and maximum current output (~200 mA) from nickel contacts device were obtained at ΔT ≈ 350 K, which would be much higher at elevated operating temperatures and employing several such thermoelectric couples. Copyright © 2016 VBRI Press.

**Keywords:** Silicides; thermoelectric device; unicycle; thermoelectric properties.

## Introduction

Clean energy necessity and depletion of fossil fuels compel the world to move towards energy harvesting via photovoltaics, thermoelectrics, wind and tidal energy renewable sources. Among these, thermoelectric generator (TEG) is a solid-state device which produces electrical energy utilizing the Seebeck effect. TEGs are becoming a more attractive option for power generation as these are stationary, noiseless and environment friendly. A large amount of energy is being wasted in power plants, industrial processes and automobiles in terms of heat and harnessing this waste heat into useful energy using thermoelectric device would enhance the efficiency of whole system. However, the TEG needs to have compatible p & n-type materials with optimum figure-of merit (ZT) and thermal stability at the operating temperatures. The constituent elements of most of thermoelectric (TE) materials like Pb, Te, Ge, rare earth elements are either toxic and/or expensive. Silicide based thermoelectric materials have proven to one of the ideal candidates for thermoelectric power generation [1-3]. Their abundance, non-toxicity and availability of compatible n & p-type TE elements promote silicides as promising futuristic thermoelectric materials [4-7]. There are quite a few studies available on the demonstration of thermoelectric power generation using Mg<sub>2</sub>Si [8-18]. The material selection for thermoelectric devices with optimum performance is crucial and depends on its thermoelectric performance, stability, ease of fabrication and cost effectiveness. Several design strategies have been adopted to fabricate silicide based thermoelectric device [8-11]. Nemoto *et al.* fabricated n-type Mg<sub>2</sub>Si unileg thermoelectric module and reported their power output characteristics [9]. Arai *et al.*

fabricated a single thermoelectric module with n-type Mg<sub>2</sub>Si & p-type NaCo<sub>2</sub>O<sub>4</sub> with nickel electrode and reported low interface resistance between legs & contacts [15]. Tohei *et al.* reported the improved bonding strength of Mg<sub>2</sub>Si with Ni electrode using aluminium foil [17]. Despite several reported studies of Mg<sub>2</sub>Si based bi-polar thermoelectric devices, a search for a p-type compatible material, which is stable and thermoelectrically compatible with n-type Mg<sub>2</sub>Si is still on. The higher manganese silicide (MnSi<sub>x</sub>) is a good thermoelectric material in view of its abundance, non-toxic nature and high resistance to oxidation [18-20]. Thus, this alloy is a low-cost, scalable and compatible p-type material for n-type Mg<sub>2</sub>Si based TEG applications. However, there is no detail study on Mg<sub>2</sub>Si-MnSi<sub>1.73</sub> thermoelectric modules, which could be a potential thermoelectric device, due to its non-toxic, earth-abundant constituent elements. In the present study, we have fabricated a unicycle thermoelectric device consisting of Mg<sub>2</sub>Si-MnSi<sub>1.73</sub> and its power output characteristics have been evaluated with two different hot end electrical contacts. The nickel contacts were used at hot & cold end in the first combination and graphite contact was used at hot end & nickel contact at cold end in second combination. The testing of silicide based thermoelectric device was carried out at a temperature difference (ΔT) of 50 to 350 K to study its output power characteristics which were correlated with the device characteristics.

## Experimental

### Materials synthesis and characterization

High purity Mg (99.95 %), Si (99.95 %), Bi (99.5 %) and Sb (99.5%) powders were weighed in proper stoichiometric proportions and blended in a high energy ball mill with

15:1 ball to powder ratio in an argon atmosphere for n-type leg fabrication. Similarly, high purity Mn (99.95 %) powders, Si (99.95 %) powders and Al (99.95 %) powders were weighed and milled in high energy ball mill with 15:1 ball to powder ratio for p-type leg preparation. The stainless steel jars and bowls are used for this purpose and milling was carried out in argon atmosphere. Both these materials were synthesized using high energy ball milling (Fritsch, Germany) followed by reaction sintering employing spark plasma sintering. These materials were sintered by spark plasma sintering process, at 1023-1173 K for 10 minutes at 60 MPa in a graphite die in vacuum. X-ray diffraction (XRD) analysis of sintered specimens was carried out with a Miniflex-II X-ray diffractometer (RigaKu, Tokyo, Japan). Analysis of the microstructure of p-type  $\text{MnSi}_{1.73}$  & n-type  $\text{Mg}_2\text{Si}$  was performed by Field Emission Scanning Electron Microscope (SUPRA V40; Zeiss, Germany). The rectangular specimens were cut from the centre of the sintered materials with a length of 10mm for Seebeck coefficient measurement. The Seebeck coefficient and electrical conductivity were measured by the four probe DC method in helium atmosphere using Ulvac- ZEM apparatus up to 873K. A circular disc specimen of 12.7mm diameter was used for thermal diffusivity measurement. The thermal diffusivity was measured by Laser Flash method using Linesis (LFA) system in vacuum upto 873K. The thermal conductivity ( $\kappa$ ) was calculated from the formula Diffusivity ( $\alpha$ )  $\times$  Specific heat ( $C_p$ )  $\times$  Density ( $\rho$ ).

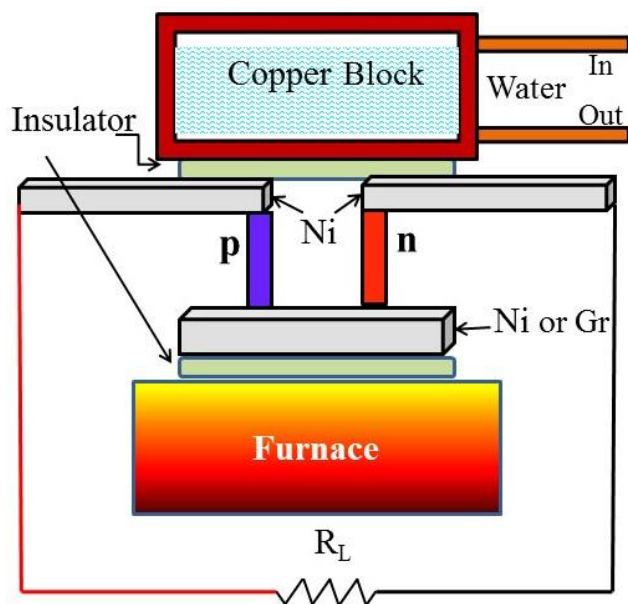


**Fig. 1.** Schematic of uni-couple thermoelectric module, consisting n-type  $\text{Mg}_2\text{Si}$  and p-type  $\text{MnSi}_{1.73}$  legs.

#### Unicouple device fabrication

The rectangular specimens were cut from the centre of the sintered material with a dimension of  $4 \times 4 \times 10$  mm for thermoelectric legs. The legs are connected by nickel contacts as shown in **Fig. 1**. The two design parameters were taken here to fabricate unicouple thermoelectric device: 1. Both hot & cold end connected by nickel plates in first one, 2. Hot end connected by graphite plates & cold end connected by nickel plates in second one. The legs and

terminals are connected using high temperature silver paste. The device setup is heated by an electric resistance heater with Inconel hot plate surface. The other side was cooled by water cooled copper block. The output voltage and current measurements were carried out at temperature difference ( $\Delta T$ ) of 50 to 350 K.

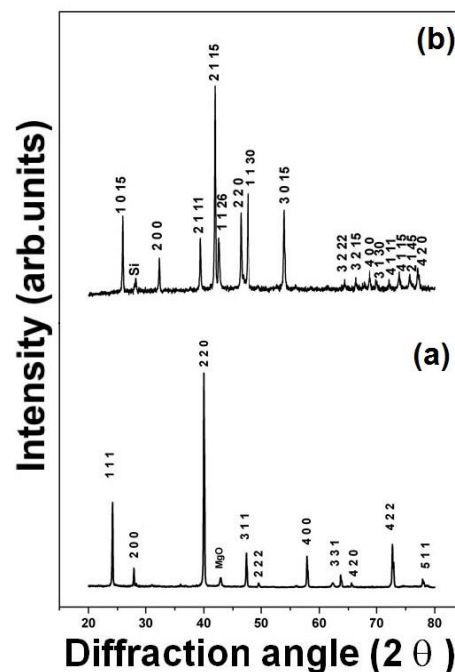


**Fig. 2.** XRD patterns of spark plasma sintered (a) n-type  $\text{Mg}_2\text{Si}$  and (b) p-type  $\text{MnSi}_{1.73}$

#### Results and discussion

XRD patterns (**Fig. 2**) of spark plasma sintered specimens reveals a single phase  $\text{Mg}_2\text{Si}$  with minor trace amount of MgO in n-type material and a single phase  $\text{MnSi}_{1.73}$  with trace amount of Si in p-type material. **Fig. 3a** shows the microstructure of the spark plasma sintered  $\text{Mg}_2\text{Si}$  (n-type) material. The microstructure evidences the equi-axed grains with round shaped morphology. **Fig. 3b** shows the microstructure of the spark plasma sintered  $\text{MnSi}_{1.73}$  (p-type) material. The microstructure analysis of both materials reveals the porosity free surface morphology.

**Fig. 4(a-d)** shows the temperature dependence of the thermoelectric transport properties of p-type  $\text{MnSi}_{1.73}$  and n-type  $\text{Mg}_2\text{Si}$ , i.e., electrical conductivity, thermal conductivity, Seebeck coefficient and figure-of-merit (ZT) respectively. **Fig. 4c** shows the Seebeck coefficient compatibility of both p & n-type material in the measured temperature range. The positive polarity indicates p-type conduction in  $\text{MnSi}_{1.73}$ , whereas negative polarity indicates n-type conduction in  $\text{Mg}_2\text{Si}$ . The electrical conductivity of the p & n-type specimen shows the decreasing trend as the temperature increases. The decrease in electrical conductivity at higher temperatures is due to lattice thermal vibrations. The temperature dependence of the thermal conductivity is shown in **Fig. 4b**. The thermal conductivity values of the p-type material show the small variations over the measured temperature range. But n-type material shows high value at room temperature whereas low stable trend at higher temperatures. At higher temperatures, decoupling of

electronic and phonons degree of freedom takes place. It is observed that the figure-of-merit of both material increase with increasing temperature. The enhanced ZT value of  $\sim 0.7$  for n-type  $\text{Mg}_2\text{Si}$  and  $\sim 0.55$  for p-type  $\text{MnSi}_{1.73}$  originated from high Seebeck coefficient values at  $\sim 873$  K. In addition to that, the study confirms the Seebeck coefficient compatibility of these synthesized p & n-type materials.

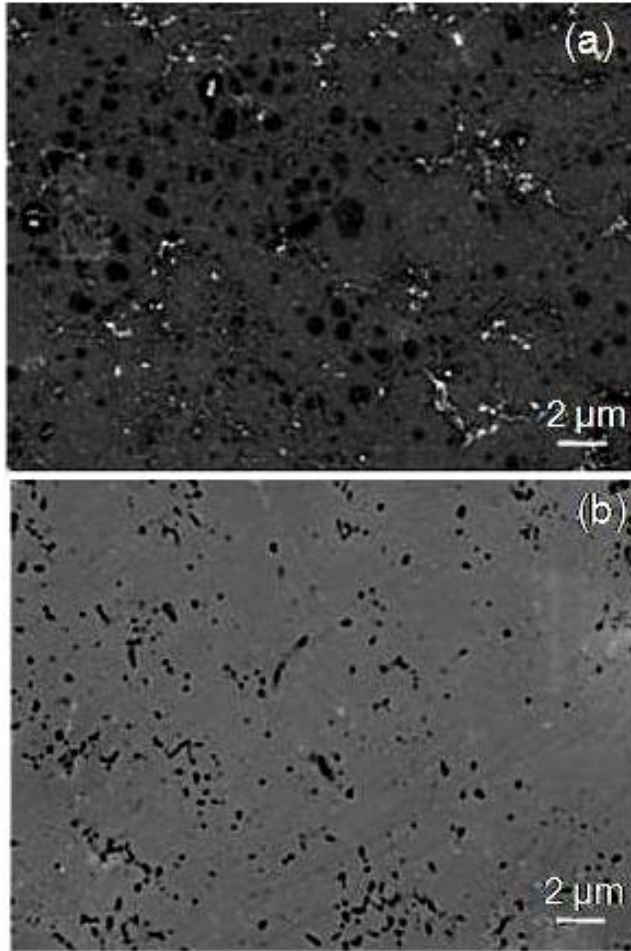


**Fig. 3.** Microstructures of spark plasma sintered (a) n-type  $\text{Mg}_2\text{Si}$  and (b) p-type  $\text{MnSi}_{1.73}$

**Fig. 5a** shows the open circuit voltage characteristics of uncouple device for the temperature difference ( $\Delta T$ ) 50 to 350 K. The high  $V_{oc}$  ( $\sim 135$  mV) is observed at  $\Delta T \approx 350$  K &  $V_{oc}$  ( $\sim 17$  mV) at  $\Delta T \approx 50$  K with nickel contacts. The graphite contacts have shown slightly lower value of  $V_{oc}$  ( $\sim 131$  mV) as compared to nickel contacts. It is also noted that the steady increase in total resistance of the system with increasing temperature. Figure 5b shows the current characteristics of uncouple device for the temperature difference ( $\Delta T$ ) 50 to 350 K. The load resistance ( $R_{load} \sim 100 \text{ m}\Omega$ ) is connected across the Ni terminals to measure device current characteristics. The value of  $I_{max} \sim 200$  mA is obtained from the Ni contacts (both hot & cold end) device and lower value of  $\sim 148$  mA with Gr (hot end) & Ni (Cold end) combinations. The output voltage coming out from this uncouple device is lower as compared to calculated value from Seebeck coefficient measurements of individual legs.

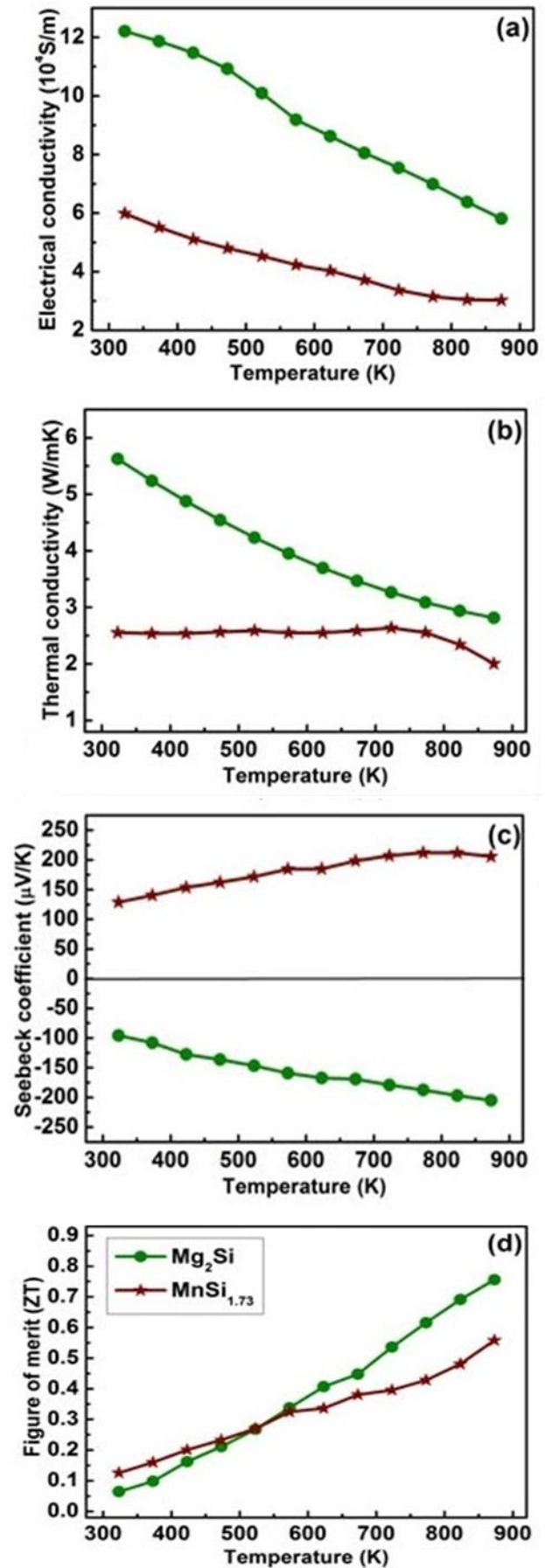


**Fig. 4.** Temperature dependence of the thermoelectric transport properties of n-type  $\text{Mg}_2\text{Si}$  and p-type  $\text{MnSi}_{1.73}$

Thermal barriers in contacts and real environmental conditions are the major concern for achieving the theoretical limits. However, the power output characteristic of uncouple device is stable for long duration working hours. There is no marginal difference in power output characteristics of both device configuration, still Ni contacts are preferred one, in terms of mechanical strength perspective. The initial results of this prototype uncouple device provide the platform for design & fabrication of actual thermoelectric module using these cost effective silicide based materials.

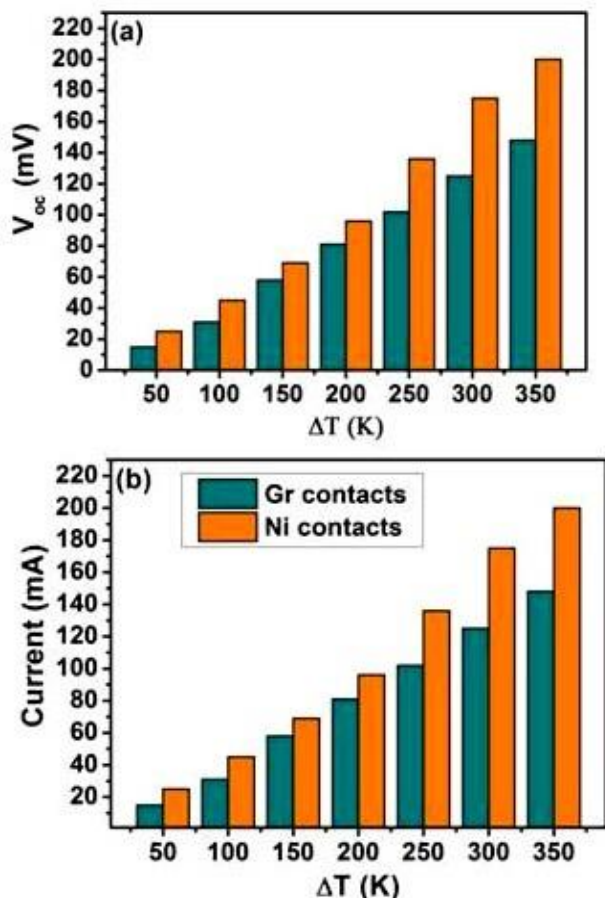


Fig. 5. Measured open circuit voltage and output current of uncouple  $Mg_2Si$  and  $MnSi_{1.73}$  thermoelectric module.

## Conclusion

We have synthesized n-type magnesium silicide and p-type higher manganese silicide material with optimized processing conditions with a ZT of  $\sim 0.7$  and  $\sim 0.55$ , respectively. The microstructural analysis evidences the material free from porosity and micro-cracks. We have fabricated a uncouple device using these thermoelectric materials p & n-type legs, which are the cost effective silicide based thermoelectric material. The maximum open circuit voltage of  $\sim 135$  mV and maximum current output 200 mA was obtained. The selection of proper contact and controlling of temperature from heat absorption and heat rejection side provides the path way to maximize the conversion efficiency. The work will be extended to study the mechanical stability and interface characteristics of electrical contacts with thermoelectric legs to improve the power output.

## Acknowledgements

This work was supported by the CSIR-TAPSUN (Network Project NWP-54) programme entitled "Novel approaches for solar energy conversion under technologies and products for solar energy utilization through networking". The authors are thankful to Metals & Alloys group members for their support & Radhey Shyam, N.K. Upadhyay, Madan Pal for technical and experimental support.

## Reference

- Zebarjadi, M.; Esfarjani, K.; Dresselhaus, M. S.; Ren, Z. F.; Chen, G.; *Energy Environ. Sci.* **2012**, 5, 5147.  
DOI: [10.1039/C1EE02497C](https://doi.org/10.1039/C1EE02497C)
- Venkatasubramanian, R.; Siivola, E.; Colpitts, T.; O'Quinn, B.; *Nature* **2001**, 413, 597.  
DOI: [10.1038/35098012](https://doi.org/10.1038/35098012)
- Snyder, G. J.; Ursel, T. S.; *Phys. Rev. Lett.* **2003**, 91, 148301.  
DOI: [10.1103/PhysRevLett.91.148301](https://doi.org/10.1103/PhysRevLett.91.148301)
- Fedorov, M. I.; Isachenko, G. N.; *Japanese J. Appl. Phys.* **2015**, 54, 07JA05.  
DOI: [10.7567/JJAP.54.07JA05](https://doi.org/10.7567/JJAP.54.07JA05)
- Liu, X.; Deng, Y. D.; Chen, S.; Wang, W. S.; Xu, Y.; Su, C. Q.; *Case Studies in Thermal Engineering* **2014**, 2, 62.  
DOI: [10.1016/j.csite.2014.01.002](https://doi.org/10.1016/j.csite.2014.01.002)
- Muthiah, S.; Pulikkotil, J.; Srivastava, A. K.; Kumar, A.; Pathak, B. D.; Dhar, A.; Budhani, R. C.; *Appl. Phys. Lett.* **2013**, 103, 053901.  
DOI: [10.1063/1.4816802](https://doi.org/10.1063/1.4816802)
- Muthiah, S.; Sivaiah, B.; Gahtori, B.; Tyagi, K.; Sivastava, A. K.; Pathak, B. D.; Dhar, A.; Budhani, R. C.; *J. Electron. Mater.* **2014**, 43, 2035.  
DOI: [10.1007/s11664-013-2944-x](https://doi.org/10.1007/s11664-013-2944-x)
- Sakamoto, T.; Iida, T.; Taguchi, Y.; Kurosaki, S.; Hayatsu, Y.; Nishio, K.; Kongo, Y.; Takanashi, Y.; *J. Electron. Mater.* **2012**, 41, 8528.  
DOI: [10.1007/s11664-012-1974-0](https://doi.org/10.1007/s11664-012-1974-0)
- Nemoto, T.; Iida, T.; Sato, J.; Oguni, Y.; Matsumoto, A.; Miyata, T.; Sakamoto, T.; Nakajima, T.; Taguchi, H.; Nishio, K.; Takanashi, Y.; *J. Electron. Mater.* **2010**, 39, 1572.  
DOI: [10.1007/s11664-010-1277-2](https://doi.org/10.1007/s11664-010-1277-2)
- Mizuno, K.; Sawada, K.; Nemoto, T.; Iida, T.; *J. Electron. Mater.* **2012**, 41, 1256.  
DOI: [10.1007/s11664-012-1911-2](https://doi.org/10.1007/s11664-012-1911-2)
- Boor, J. D.; Gloanec, C.; Kolb, H.; Sottong, R.; Ziolkowski, P.; Muller, E.; *J. Alloys Compd.* **2015**, 632, 348.  
DOI: [10.1016/j.jallcom.2015.01.149](https://doi.org/10.1016/j.jallcom.2015.01.149)
- Kajitani, T.; Ueno, T.; Miyazaki, Y.; Hayashi, K.; Fujiwara, T.; Ihara, R.; Nakamura, T.; Takakura, M.; *J. Electron. Mater.* **2014**, 43, 1993.  
DOI: [10.1007/s11664-013-2933-0](https://doi.org/10.1007/s11664-013-2933-0)
- Kadhim, A.; Hmood, A.; Hassan, H. A.; *Journal of Physics: Conf. Ser.* **2013**, 431, 012002.  
DOI: [10.1088/1742-6596/431/1/012002](https://doi.org/10.1088/1742-6596/431/1/012002)
- Gupta, R. P.; McCarty, R.; Sharp, J.; *J. Electron. Mater.* **2014**, 43, 1608.  
DOI: [10.1007/s11664-013-2806-6](https://doi.org/10.1007/s11664-013-2806-6)
- Arai, K.; Matsubara, M.; Sawada, Y.; Sakamoto, T.; Kineri, T.; Kogo, Y.; Iida, T.; Nishio, K.; *J. Electron. Mater.* **2012**, 41, 1771.  
DOI: [10.1007/s11664-012-2036-3](https://doi.org/10.1007/s11664-012-2036-3)
- Nakamura, S.; Mori, Y.; Takarabe, K.; *J. Electron. Mater.* **2014**, 43, 2174.  
DOI: [10.1007/s11664-014-3000-1](https://doi.org/10.1007/s11664-014-3000-1)
- Tohei, T.; Fujiwara, S.; Jinushi, T.; Ishijima, Z.; *IOP Conf. Ser.: Materials Science and Engineering* **2014**, 61, 012035.  
DOI: [10.1088/1757-899X/61/1/012035](https://doi.org/10.1088/1757-899X/61/1/012035)
- Luo, W.; Li, H.; Yan, Y.; Lin, Z.; Tang, X.; Zhang, Q.; Uher, C.; *Intermetallics* **2011**, 19, 404.  
DOI: [10.1016/j.intermet.2010.11.008](https://doi.org/10.1016/j.intermet.2010.11.008)
- Sadia, Y.; Gelbstein, Y.; *J. Electron. Mater.* **2012**, 41, 1504.  
DOI: [10.1007/s11664-012-1936-6](https://doi.org/10.1007/s11664-012-1936-6)
- Ponnambalam, V.; Morelli, D.T.; *J. Electron. Mater.* **2011**, 41, 1389.  
DOI: [10.1007/s11664-011-1843-2](https://doi.org/10.1007/s11664-011-1843-2)

